13th World Conference on Earthquake Engineering
Vancouver, B.C., Canada
August 1-6, 2004
Paper No. 1552

NUMERICAL INVESTIGATION OF SEISMIC ISOLATION FOR SINGLE-TOWER CABLE STAYED BRIDGES

Charles B. CHADWELL[1], Stephen A. MAHIN[2], Gregory L. FENVES[3]

SUMMARY

Recent earthquakes have demonstrated the vulnerability of cable-stayed bridges to near-fault earthquake excitation. The end span connections of the Higashi-Kobe cable-stayed bridge fractured during the Hyogoken-Nanbu (Kobe) Earthquake in 1995 causing moderate damage to the overall system [1,2]. The end spans of the Chi-Lu cable-stayed bridge rose vertically out of their transverse shear keys during the 1999 Chi-Chi earthquake in Taiwan resulting in extensive damage to the non-ductile superstructure at the superstructure to central pylon connection [3].

This paper explores isolation for protecting these structural systems due to large magnitude, near source seismic events. Using isolation devices under the central pylon in conjunction with isolation devices at the end span connections, the complete system can be isolated and the superstructure can be protected. This paper focuses on issues related to isolating the bridge in the transverse direction. This form of isolation minimizes the demands to both the superstructure and substructure elements. Flexible bearings are provided connecting the end spans to the substructure and the pylon base to the foundation. These isolator groups are tuned such that a vibration mode is created where the superstructure is engaged primarily in translation.

This paper develops the required relationship between the end span and pylon-foundation flexible connections to optimize the effectiveness of the isolation system. Furthermore, analytical results for a fixed base, fixed end, moderate span, single-tower cable-stayed bridge are compared with results from the pylon isolation system for varying isolation periods using simulations with large magnitude near-fault ground motions. Conclusions are drawn on the overall all effectiveness of this method of isolation as compared with the traditional fixed base system. Results will show that isolation of the entire system is a viable option for the reduction of seismic damage.

[1] Assistant Professor, Civil and Environmental Engineering, California Polytechnic State University, San Luis Obispo, CA, USA: chadwell@calpoly.edu
[2] Professor, Civil and Environmental Engineering, University of California, Berkeley, CA, USA: mahin@ce.berkeley.edu
[3] Professor, Civil and Environmental Engineering, University of California, Berkeley, CA, USA: fenves@ce.berkeley.edu

INTRODUCTION

Currently, when seismic isolation is used to mitigate damaging effects due to earthquake excitation on moderate span cable-stayed bridges, it is typically provided at the end span connections and between the superstructure and central pylons. With this method of isolation, costs can be substantially increased when an 'I' shaped pylon is used due to the increased overall superstructure width required to provide displacement capacity in the transverse direction between the superstructure and the pylon. In addition, this isolation scheme does not directly protect the pylons from seismic demands.

By providing the isolation mechanism at the base of the pylon along with isolation at the end spans, both the superstructure and pylons can be protected while the forces transmitted to the pylon foundation can be greatly reduced. With this mechanism of isolation, it is important to calibrate the effective stiffness of the isolation devices at the end spans and under the pylons with the overall dynamic properties of the bridge. This paper derives the relationship between the stiffness of the flexible bearing devices at the pylon-foundation connection with the stiffness of the bearing devices at the end span superstructure-substructure connection for a given target isolation period. Furthermore, the seismic mitigating effects of this isolation system are compared to the fixed base, fixed end counterpart for varying target isolation periods. The example structure used for evaluation of this system is the Chi-Lu Bridge located in central Taiwan.

THE CHI-LU BRIDGE

The Chi-Lu bridge was significantly damaged in the 1999 Chi-Chi Earthquake. Results of an extensive analytical and field study with the Chi-Lu cable-stayed bridge revealed that during the 1999 Chi-Chi earthquake, the end span of the Chi-Lu bridge rose vertically out of their shear key transverse restraints resulting extensive damage [4]. Analytical results show that with a fixed base model, significant damage occurs if the end spans are allowed to release during seismic excitation. However, more effectively restraining the end spans in the transverse direction, large demands are placed on the end span connections as well as the substructure supports. With a combination of flexible end span connections and flexible bearings placed between the central pylon and the foundation, significant seismic demand reductions can be attained. Issues related to isolation for response in the longitudinal direction are discussed elsewhere [4].

The Chi-Lu Bridge is a symmetric single tower cable-stayed structure supporting two 120.0m span segments (Figure 1). The central tower (P12) is 76.0m high extending 56.0m above the main span deck elevation. Each end of the main span is supported by a two-column transversely-orientated bent, P11 (north) and P13 (south). The box girder is cast-in-place concrete supported by two rows of 17 high-strength cable stays on each side of the central tower - 68 cables total.

Fixed Base Model

The base of the end piers are considered fully restrained against rotation because of the large difference in cross-section size between the pier columns and pile extensions. Furthermore, the pile extensions at the P11 and P13 piers are embedded in 15m of sandstone. The soil is very stiff and thus this support is also assumed restrained against translation in the three orthogonal directions.

The central pylon of the Chi-Lu bridge rests atop a pile cap housing 72 - 15m long piles embedded 13m into sandstone. Preliminary analysis with a varying foundation translational and rotational soil spring stiffness showed little influence of the soil flexibility on the overall bridge response. Hence, the boundary conditions are modeled with translational and rotational fixity in the three orthogonal directions.

The end spans of the Chi-Lu Bridge are connected to the end span substructure supports with a shear key type connection that provides restraint in the transverse direction while allowing displacement freedom in

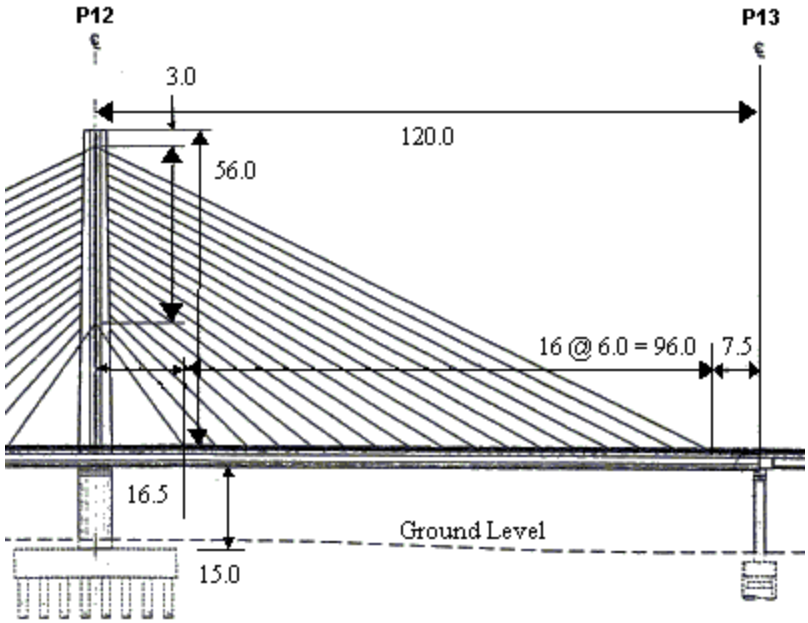

Figure 1 - Chi-Lu bridge side view in unit of meters (Courtesy of T. Y. Lin International).

the longitudinal direction. In the vertical direction, the substructure provides restraint in the downward direction; however, the end spans are free to move in the upward direction. Transverse restraint at the end spans was provided by the shear key only so long as the vertical displacement did not exceed 25cm. Release of the displacement restraint after exceeding the height of the shear key largely contributed to damage in Chi-Chi Earthquake.

The overall Chi-Lu Bridge structural model is discretized as shown in Figure 2 with structural masses lumped at the nodes.

Pylon Base Isolation Model

In the proposed Pylon Isolation Model, flexible bearings are considered at the pylon-foundation connection in conjunction with flexible bearings at the end span-substructure connection. Because of the large foundation sizes typical of bridges of this type, placement of flexible bearing devices between the pylon foundation and the pile cap is feasible (Figure 3).

To create an effective isolation system in the transverse direction, the stiffness of the isolation devices under the central pylon must be tuned relative to the stiffness of the isolation devices used to connect the end spans to the end span substructure supports. The tuning of these two sets of bearings is done to minimize strong axis bending of the superstructure.

To begin, it is of interest to consider the bounding cases for dynamic response of the fixed base structure where the end spans are transversely restrained and where they are transversely free. The first transverse modal response between these two cases for the Chi-Lu Bridge shows only a slight difference in period and virtually no change in mode shape (Figure 4). The second transverse modal response, however, reveals a significant difference (Figure 5). By inserting flexible bearing devices between the end spans and the end span supports, and varying the bearing stiffness from infinity (as is the case when the end spans are transversely restrained) to zero (as is the case when the end spans are transversely free), the dynamic behavior is

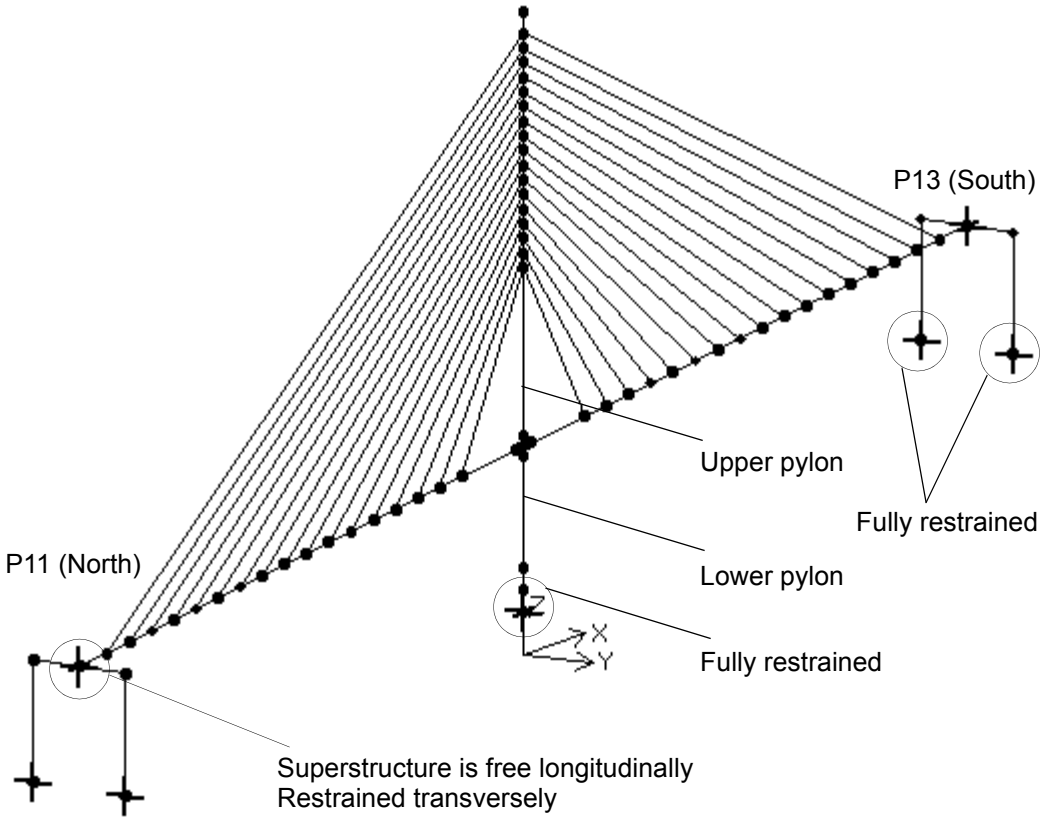

Figure 2 - Structural model of the Chi-Lu cable-stayed bridge.

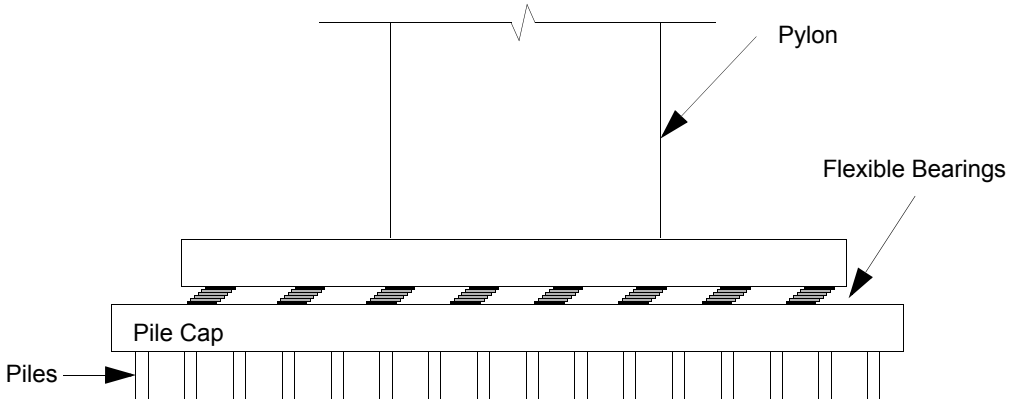

Figure 3 - Location of proposed flexible bearings devices at the pylon-foundation connection.

bounded between the modal response of the transverse displacement restrained and the transverse displacement free systems. To create an effective isolation system that minimizes transverse demands on the superstructure, the relationship between the end span and the pylon-foundation connection bearing flexibilities needs to be found such that the superstructure is engaged in uniform translation. To achieve this, modal

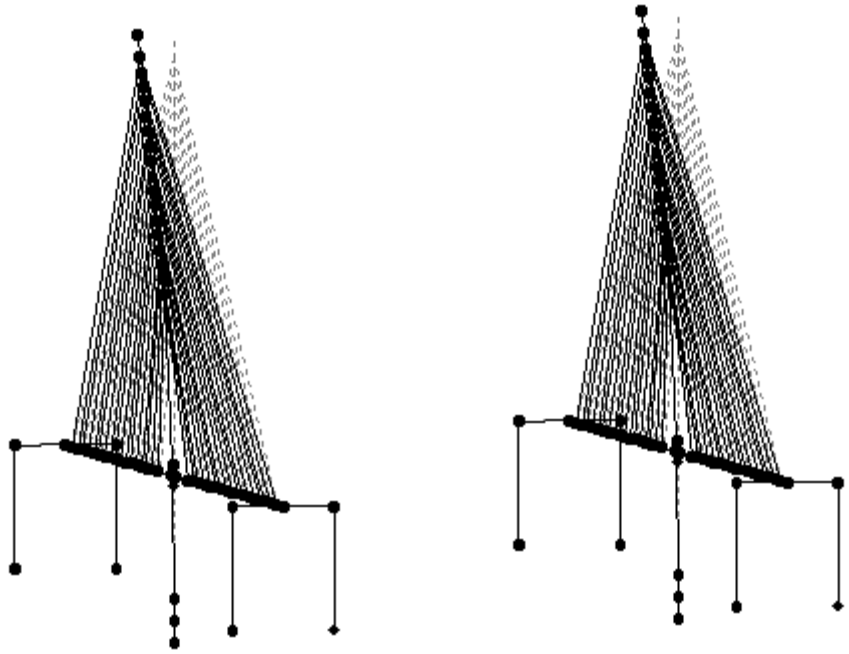

Figure 4 - First mode of vibration with (2.05 sec.) and without (2.10 sec.) the end spans restrained.

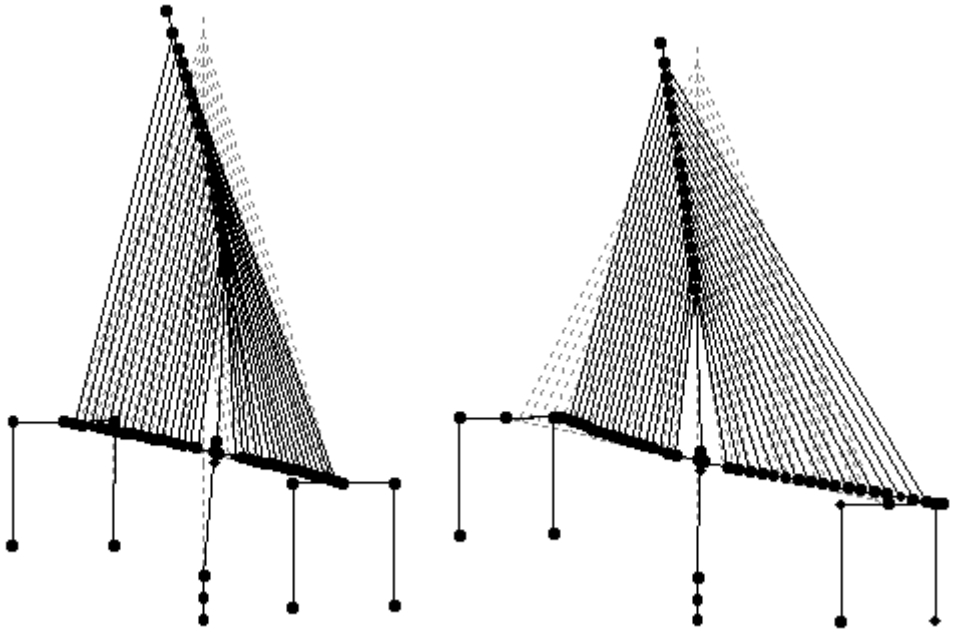

Figure 5 - Second transverse mode of vibration with ends restrained transversely - 0.53sec (left). Second transverse mode of vibration with ends free transversely - 1.33sec (right).

analysis will be performed combining the second transverse modes of vibration for the ends free and ends restrained cases in generalized coordinates.

Using a simplified two-degree-of-freedom model in generalized coordinates, two shape functions can be described. The first shape function (Shape 1) engages only the end span with the superstructure in transverse bending (Ψ_{2a}). The second shape function (Shape 2) engages only the pylon with the superstructure in transverse bending (Ψ_{2b}). The generalized shape functions are shown in Figure 6 where EI_s and m_s are

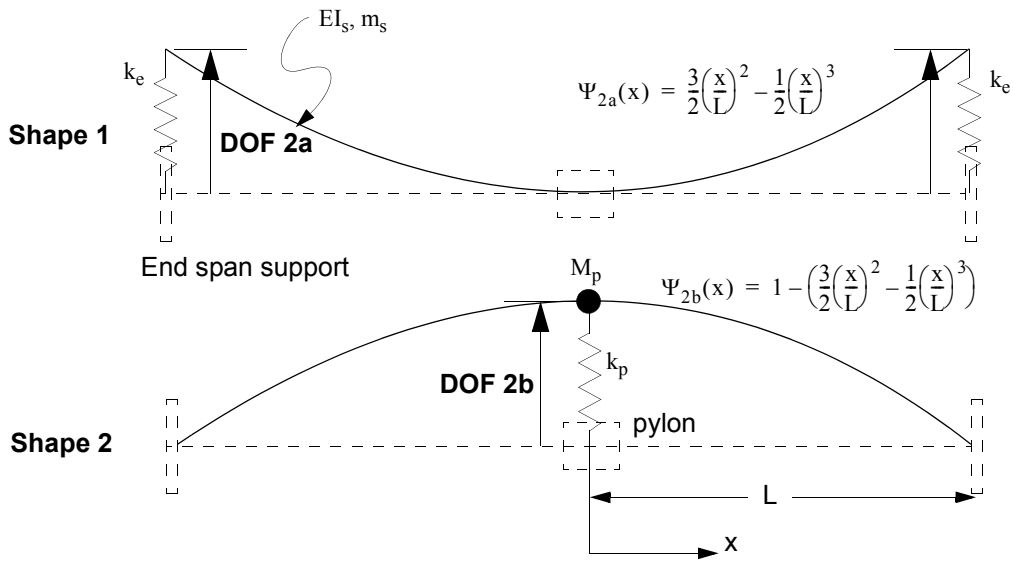

Figure 6 - Plan view of generalized shape functions showing superstructure displacement interpolation.

the bending stiffness per unit length and mass per unit length of the superstructure, respectively. The functions are symmetric, cubic polynomials representing the displaced shape of a unit load at the generalized degrees of freedom. Because the result of this derivation will be a translational mode of the superstructure, the pylon is assumed relatively inflexible and lumped as a concentrated mass (M_p) with stiffness equal to the stiffness of the bearing devices under the central pylon (k_p).

With the two generalized degrees of freedom for the superstructure, the eigenvalue problem can be expressed in terms of the generalized stiffness (k), generalized mass (m), modal frequency of vibration (ω_n), and modal coordinates (ϕ):

$$\begin{bmatrix} k_{11} & k_{12} \\ k_{21} & k_{22} \end{bmatrix} \begin{bmatrix} \phi_1 \\ \phi_2 \end{bmatrix} = \omega_n^2 \begin{bmatrix} m_{11} & m_{12} \\ m_{21} & m_{22} \end{bmatrix} \begin{bmatrix} \phi_1 \\ \phi_2 \end{bmatrix}$$

where the generalized mass and stiffness values can be found from integration of the shape functions as follows:

$$k_{11} = 2EI_s\left(\int_0^L \frac{d^2}{dx^2}[\Psi_{2a}(x)]^2 dx\right) + 2k_e = \frac{6EI_s}{L^3} + 2k_e \qquad m_{11} = 2\int_0^H m_s[\Psi_{2a}(x)]^2 dx + m_{eff} = \frac{33}{70} m_s L$$

$$k_{12} = k_{21} = 2EI_s\left(\int_0^L \frac{d^2}{dx^2}[\Psi_{2a}(x)\Psi_{2b}(x)]dx\right) = -\frac{6EI_s}{L^3} \qquad m_{12} = m_{21} = 2\int_0^H m_s\Psi_{2a}(x)\Psi_{2b}(x)dx = \frac{39}{140}m_sL$$

$$k_{22} = 2EI_s\left(\int_0^L \frac{d^2}{dx^2}[\Psi_{2b}(x)]^2dx\right) + k_p = \frac{6EI_s}{L^3} + k_p \qquad m_{22} = 2\int_0^H m_s[\Psi_{2b}(x)]^2dx + M_p = \frac{34}{35}m_s L + M_p$$

Given that the mode shape of interest is one that results in uniform translation of the superstructure, the modal coordinates are: ϕ_1=1 and ϕ_2=1. With the modal coordinates known, the eigenvalue problem can be expanded to two simultaneous equations. Then, upon substitution of the generalized mass and stiffness coordinates, and eliminating the unknown frequency, a relationship between the stiffness of the pylon-foundation flexible bearing devices and the end span-substructure flexible bearing devices can be found. The relation is presented in terms of the total mass of the superstructure (M_s) and the total mass of the central pylon (M_p):

$$k_e = \frac{3}{2} \cdot k_p \cdot \frac{M_s}{5M_s + 8M_p}$$

The result presented above assumes an inflexible pylon. To develop an equation involving an estimation of the isolation period of vibration (T) with uniform translation of the superstructure, the actual flexibility of the central pylon must be included. This is done by using another simplified two-degree-of-freedom system relating the pylon deformation mode with the superstructure mode in uniform translation. DOF 1 is the generalized mode shape of the pylon and DOF 2 is the generalized mode shape describing the superstructure under uniform translation (Figure 7). The effective mass (m_{peff}) and stiffness (k_{peff}) of the pylon can be

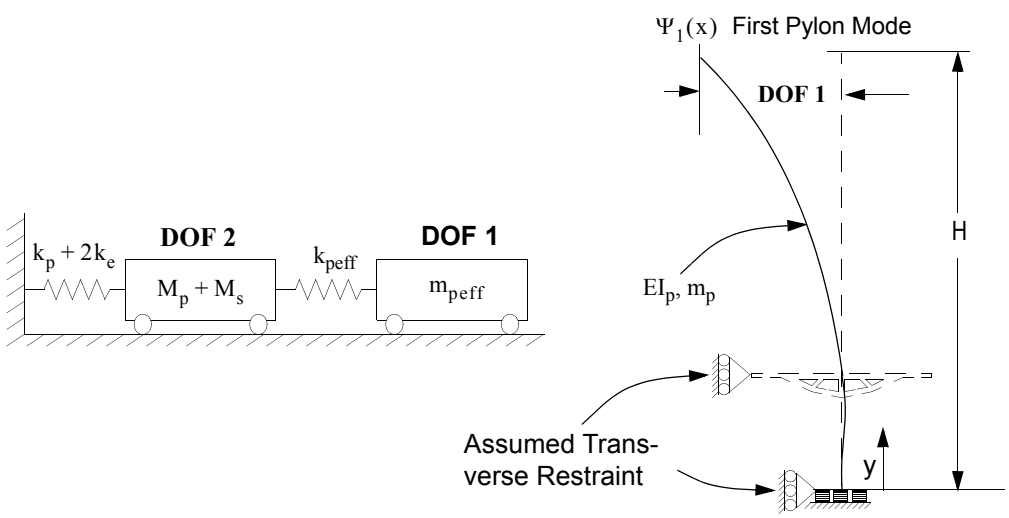

Figure 7 - Simplified two degree of freedom model coupling the superstructure with the pylon (left) and the elevation view of the generalized shape function for the pylon (right).

found from the first transverse mode of vibration of the central pylon with a fixed base and transverse restraint applied at the superstructure level.

Forming and solving the eigenvalue problem for this two-degree-of-freedom system gives two solutions. The first mode and corresponding period is the one in which the superstructure is engaged in translation (the isolation period). The second mode and corresponding period contains the pylon subject to asymmetric motion (T_2) similar to the pylon mode shown in Figure 7. Taking the solution from the first period of vibration, and rewriting it in terms of the isolation period (T) gives the following relationship between the approximate isolation period (with the superstructure engaged primarily in translation) and the pylon-foundation connection stiffness:

$$k_p = \frac{1}{2} \cdot \frac{\pi^2}{T^2 - T_2^2}\left[\left(1 + \frac{m_{eff}}{M_p + M_s}\right) - \left(\frac{T_2}{T}\right)^2\right](5M_s + 8M_p)\ , \qquad T > T_2$$

$$T_2 = 2\pi\sqrt{\frac{m_{eff}}{k_{eff}}}$$

where T_2 can be found from dynamic analysis of the transversely restrained pylon system representing the generalized DOF 1 (the pylon mode). The assumption in solving the eigenvalue problem and choosing the first solution are such that the isolation period is greater than the transverse mode of vibration that engages the pylon (T_2). Hence, the above result is valid for T greater than T_2.

Using the results presented above, for a given target isolation period, the required end span stiffness and pylon isolation device stiffness can be estimated. These will tend to produce a response under transverse vibration where the bridge superstructure undergoes minimal strong axis bending.

Pylon Isolation Model Verification

To verify the result derived above between the isolation period, end span connection stiffness, and pylon-foundation connection stiffness, modal analyses are performed on a range of target isolation periods (2.0sec - 7.0sec) with the Chi-Lu Bridge. The properties representing the Chi-Lu Bridge used in the numerical investigation are: $M_p = 4.1\text{x}10^6$kg, $M_s = 9.0\text{x}10^6$kg, $T_1 = 1.87$sec, $m_{eff} = 0.45\text{x}10^6$kg.

Table 1 shows the target periods, actual periods (first and second mode), pylon connection stiffness, end span stiffness, period errors (between the first transverse modal period and the target isolation period), and shape errors. The period errors are given as the absolute value of the difference between actual first mode periods and the assumed target values normalized by the actual first mode periods and are reported as a percent difference. The shape errors are given as the absolute value of the difference between the modal coordinate of the end span and the modal coordinate of the superstructure at the pylon normalized by the modal coordinate at the end span and reported as a percent error (Figure 8). A shape error of zero corresponds to uniform translation of the superstructure with center and end spans moving completely in phase.

Results presented show very good comparison between the actual versus calculated isolation periods with all errors less than 5%. Furthermore, the similarity between modal values at the end spans and at the pylon-superstructure connection suggest limited superstructure bending.

It is of interest to note that the period of vibration of the pylon mode (second transverse mode) does not vary considerably for a wide range of end span stiffness (and calibrated pylon-foundation stiffness). For long isolation periods, the second modal period appears to asymptotically approach the period of the restrained pylon mode ($T_1 = 1.87$sec) as described in Figure 7. This, in turn, suggests that a target isolation period can be chosen without significant variation to the other dynamic characteristic.

Table 1 - Results of varying isolation stiffness analyses.

Target Period (sec)	1st Modal Period (sec)	2nd Modal Period (sec)	Pylon Connection Stiffness (kN/m)	End Span Stiffness (kN/m)	Period Error (%)	Shape Error (%)
2.0	2.08	1.55	122138	21194	3.8	8.3
2.2	2.25	1.66	89121	15465	2.2	0.9
2.4	2.44	1.71	72469	12575	1.6	0.0
2.6	2.62	1.73	60827	10555	0.8	0.8
2.8	2.78	1.74	52000	9023	0.7	1.6
3.0	3.00	1.76	45050	7817	0.0	1.0
3.2	3.17	1.76	39444	6844	0.9	1.5
3.4	3.40	1.77	34844	6046	0.0	1.0
3.6	3.56	1.77	31015	5382	1.1	1.3
3.8	3.77	1.78	27790	4822	0.8	1.1
4.0	3.93	1.78	25048	4346	1.8	1.3
5.0	4.91	1.79	15969	2771	1.8	0.8
6.0	5.78	1.79	11070	1921	3.8	0.8
7.0	6.91	1.80	8124	1410	1.3	0.3

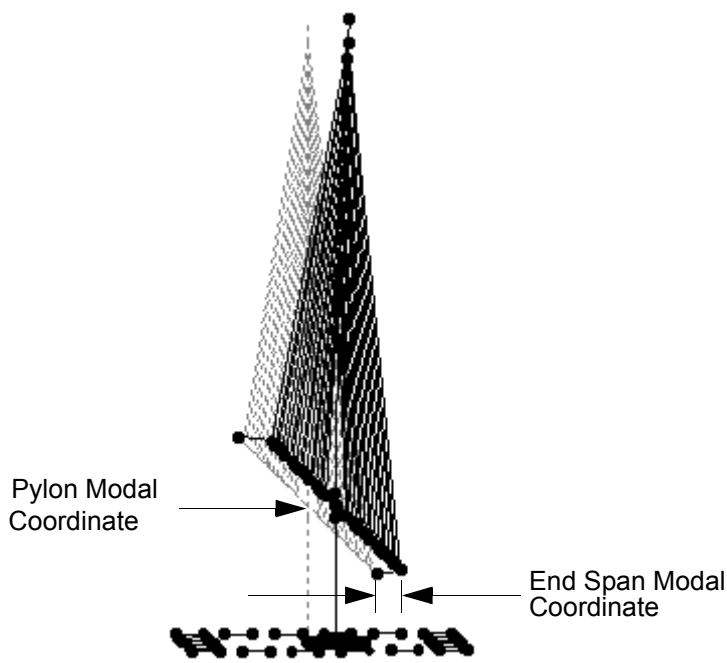

Figure 8 - First transverse mode of vibration with target period of 4.0sec.

RESULTS

To investigate the effects of calibrated isolation on the Chi-Lu Bridge subjected to earthquake excitation, three ground motions are selected (Figure 9): LP89lpc (Los Gatos, LGPC, 000, Loma Prieta Earthquake, 1989), NR94rrs (Rinaldi Receiving Station, 228, Northridge Earthquake, 1994) and

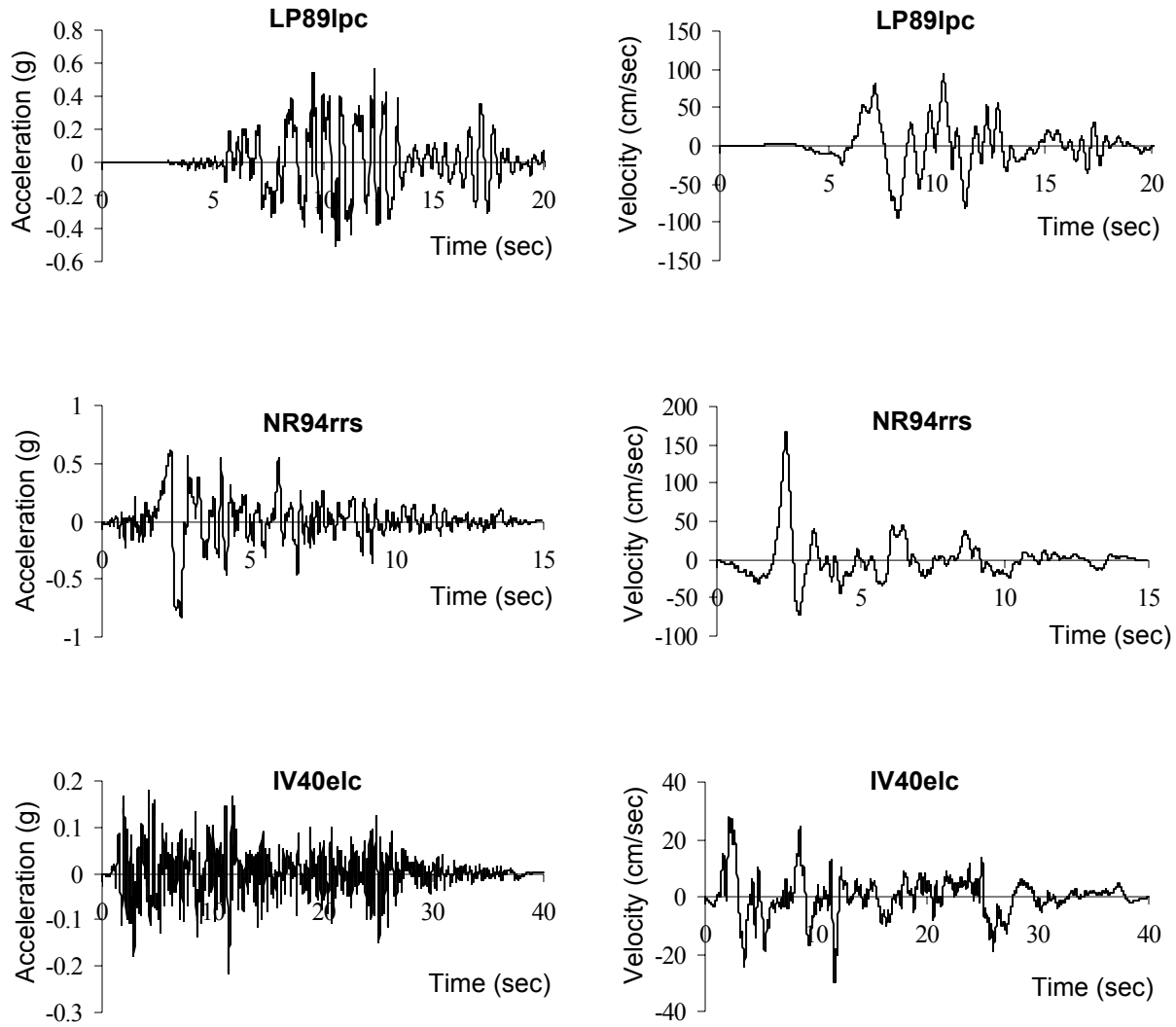

Figure 9 - LP89lpc (top), NR94rrs (center), and IV40elc (bottom) acceleration and velocity time histories.

IV40elc (El Centro Array #9, El Centro Earthquake, 1940). The records used were extracted from the PEER Strong Motion Database [5]. The high velocity LP89lpc record is chosen because it produces the largest transverse superstructure bending demand with the end spans restrained in the transverse direction of all high velocity records considered in a detailed study of the fixed base model. The high velocity NR94rrs record is chosen because it produces the largest superstructure bending demand with the end spans free in the transverse direction. The IV40elc was chosen because it is a commonly used low velocity record.

Three dimensional time history analyses with geometric nonlinearity using Opensees [6] are performed on the Pylon Isolation Model with varying target isolation periods ranging from 2.0sec - 5.0sec in increments of 0.2sec. Simulation results from these analyses are compared with results from analyses with the fixed end, fixed base model. Comparisons are shown for the peak strong axis superstructure demand-capacity

ratios, the peak transverse pylon bending demand-capacity ratios, and the peak end span displacement demands.

Superstructure Demands

Simulation results with the ground motions used show that strong axis superstructure bending demands are substantially less (Figure 10) than demands found from simulations with the end spans transversely

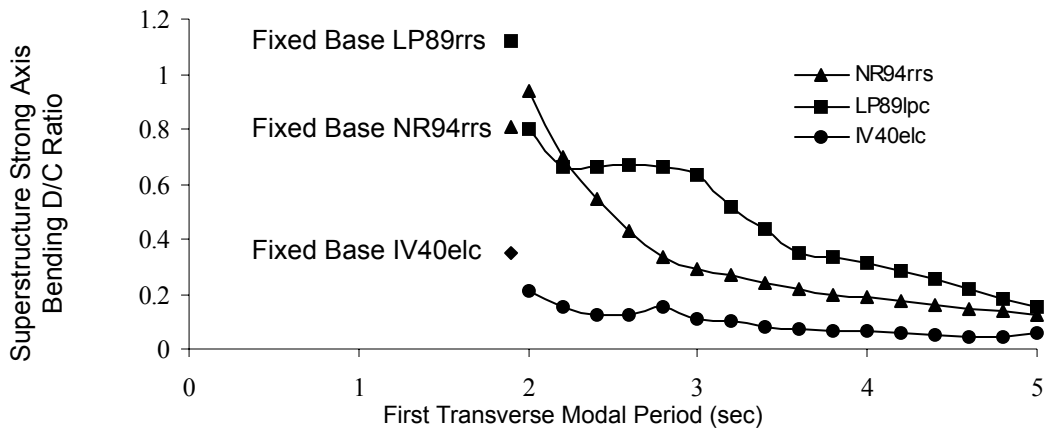

Figure 10 - Peak transverse superstructure bending demands versus first modal period for the LP89lpc, NR94rrs, and IV40elc ground motions.

restrained. Furthermore, Figure 10 shows that strong axis bending demands are reduced with increasing isolation periods for the high velocity short pulse (NR94rrs), long pulse (LP89lpc), and far field (IV40elc) ground motions.

Central Pylon Demands

The peak transverse bending demands of the central pylon above the superstructure (Figure 11) reveals sim-

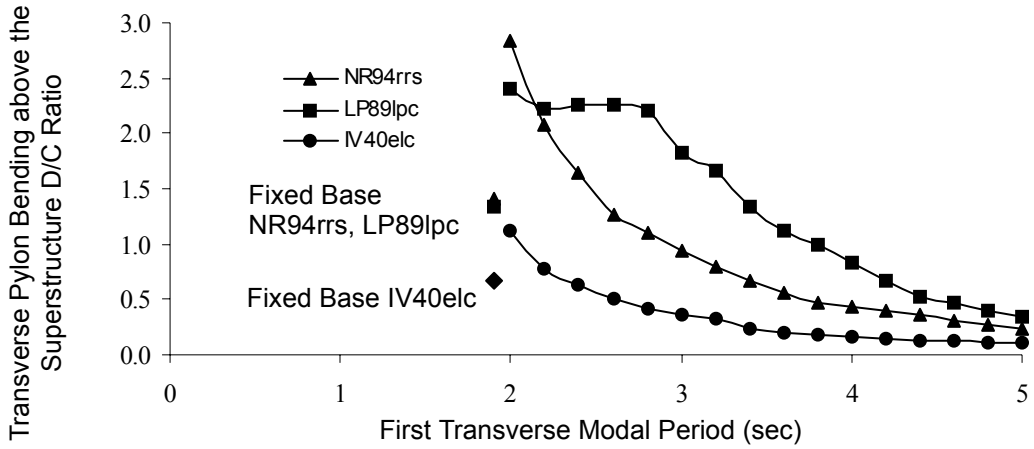

Figure 11 - Peak transverse pylon bending demands above the superstructure versus first modal period for the LP89lpc, NR94rrs, and IV40elc ground motions.

ilar trends as those observed with strong axis bending demands of the superstructure. Increasing the isola-

tion period decreases the demands for the ground motions considered. However, isolation in the shorter periods (less than 3.0sec) shows an increase in the pylon bending demands over the end span restrained model for the three ground motions considered.

Transverse bending demands of the pylon below the superstructure and above the pile cap are also greatly reduced with the introduction of flexible bearings at both the end span and pylon-foundation connections as compared with fixed end, fixed base model (Figure 12). For the range of periods considered and two of the

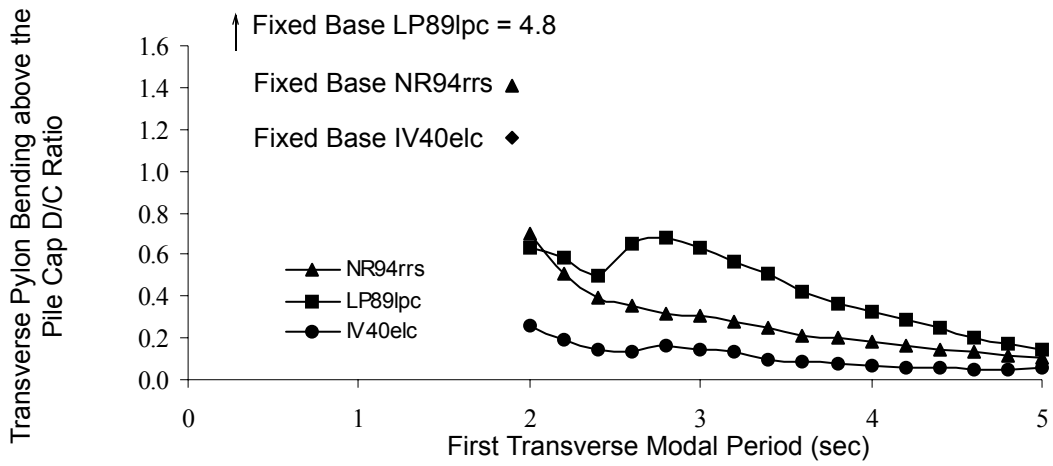

Figure 12 - Peak transverse pylon bending demands above the pile cap versus first modal period for the LP89lpc, NR94rrs, and IV40elc ground motions.

ground motions analyzed, there is a reduction of demands with increasing periods. Analysis with the LP89lpc, however, shows an increase in demands near the ground motion pulse period (3.0sec) of this near-fault pulse type ground motion record. The pulse period for this ground motion is defined in Makris and Black [7]. Because the isolation period closely matches the ground motion pulse period of 3.0sec, this amplification in demand is not unexpected.

End Span Displacement

The pulse period of the LP89lpc ground motion is also evident in the peak end span transverse displacement versus isolation period as shown in Figure 13. The NR94rrs and IV40elc ground motions show relatively constant end span peak displacements from the shorter to longer period systems, whereas the LP89lpc shows a large amplification near the ground motion pulse period. Again, this result is not unexpected for reasons described above.

DISCUSSION

Pylon Instability

Because flexible bearings are considered at the base of the pylon rather than a more traditional location, the possibility of overturning and pylon instability can be an issue. For this reason, the potential for overturning and instability of the central pylon must be considered.

Typically flexible bearing devices do not perform well under high tensile demands. For this reason, these bearing devices should be protected against tension. Assuming a lower bound where the bearing devices are not capable of taking any tension, pylon stability can be investigated. Assuming the bearing devices are distributed uniformly between the pylon foundation and the pile cap, then the overturning moment causing

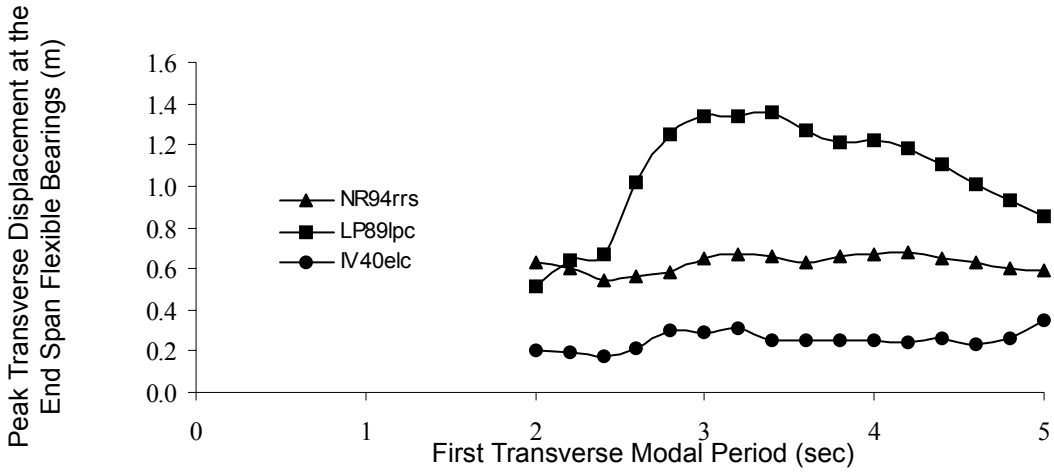

Figure 13 - Peak transverse end span displacements versus first modal period for the LP89lpc, NR94rrs, and IV40elc ground motions.

instability will theoretically occur when the applied moment (M) exceeds the axial force (P) times one-half the pile cap width (R). Tension, however, will occur when the applied moment exceeds one-sixth of the pile cap width times the axial force. These cases are shown schematically in Figure 14.

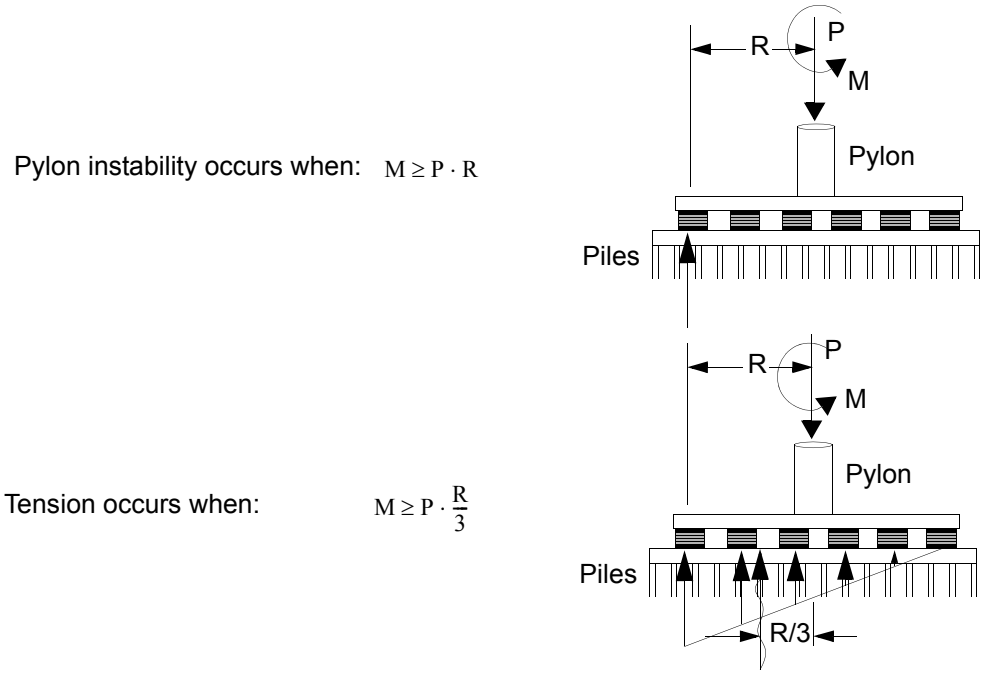

Figure 14 - Schematic showing pylon instability and tension in the bearing devices.

To prevent pylon instability from occurring as well as tension in the flexible bearings, the pylon yield moment can be used to capacity protect the system. Figure 15 shows two interaction diagrams for the Chi-Lu Bridge central pylon with the gravity load and trajectories for R/3 (the tension case) and R (the instability

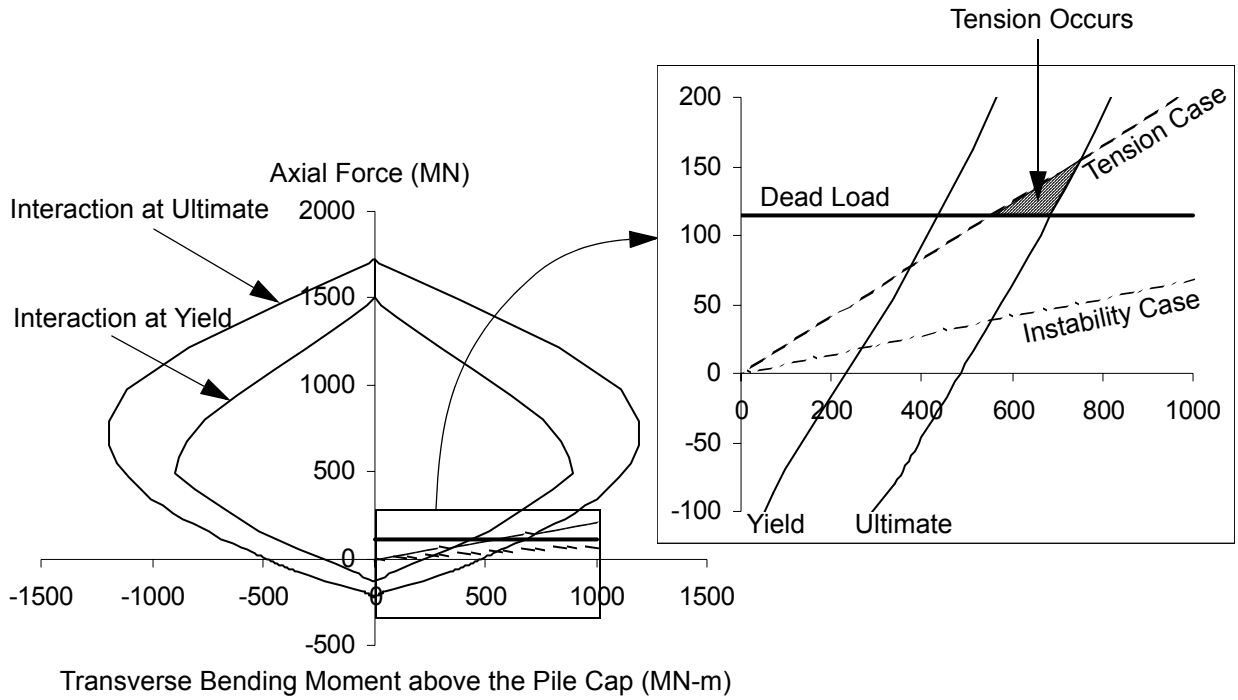

Figure 15 - Axial force-bending moment interaction diagrams for the Chi-Lu Bridge central pylon.

case). The interaction diagrams are calculated for the yield and ultimate axial force-moment interaction surfaces using XTRACT [8]. Results show that instability is sufficiently protected by the strength of the central pylon whereas some tension may occur after the pylon yields in flexure but before it reaches its ultimate capacity.

CONCLUSION

Cable stayed bridges can be vulnerable to damage from near-fault type ground motions from large magnitude earthquakes. Previous research has suggested that allowing the end span to displace can result in extensive damage due to pounding and excessive superstructure strong axis bending demands. Restraining the end spans can be difficult due to the large forces generated from near fault events. Traditional isolation can be costly for simple, moderate span, cable stayed bridges with 'I' shaped pylons due to the required displacement demands around the central pylon.

Because of the large foundations typically required for bearing, an isolation layer can be provided between the pylon and the foundation thereby limiting the transmission of the force between the pylon and the foundation. However, isolation in this location alone is not sufficient. To limit seismic bending demands to the superstructure, tuned flexible bearing devices are also required at the end span superstructure-substructure connections. With the tuned isolation system, the isolation period can be chosen and the required stiffness of these connection can be found using properties of the cable stayed bridge.

Results show the tuned pylon isolation system can reduce strong axis bending demands to the superstructure as well as transverse seismic bending demands to the central pylon. The greatest reduction, however, is to the pylon bending demands above the pile cap for the near fault type ground motions. Finally, it is pointed out that overturning and instability of this system is not possible because the overturning moment is capacity

protected by the central pylon. However, results do show that some tension my occur if the ground motion is sufficiently large enough to cause significant flexural yielding of the central pylon. However, because of the reduction in demands shown from analyses with the LP89lpc, NR94rrs, and IV40elc ground motions to below 80% of capacity for all isolation periods considered, tension would not be expected. Thus, it is clear that isolation under the central pylon presents a viable alternative to traditional isolation systems for simple, moderate span, cable stayed bridges with 'I' shaped pylons.

Additional information on the results presented herein, including the effectiveness of isolation in the longitudinal direction by be found in [4].

REFERENCES

1. Gheorghiu, C., F. Yamazaki, T. Ganev, H. Ishizaki. "Seismic Response of the Higashi-Kobe Bridge during the 1995 Hyogoken-Nanbu Earthquake." Bulletin of Earthquake Resistant Structure Research Center; 31, March (1998): 23-39.
2. Gheorghiu, C., F. Yamazaki, H. Ishizaki. "Seismic Response of the Higashi-Kobe Bridge during the 1995 Hyogoken-Nanbu Earthquake", The 10th Earthquake Engineering Symposium (1998); Vol. 2, Paper No. E2-18: 1791-1796.
3. Chadwell, C.B., G.L. Fenves, S.A. Mahin. "Cable-Stayed Bridge Behavior under Earthquake Excitation - A Case Study", The 7th National Conference on Earthquake Engineering (2002); Paper No. 37.
4. Chadwell, C.B. "Seismic Response of Single-Tower Cable Stayed-Bridges", Dissertation (2003), University of California, Berkeley.
5. PEER, Pacific Earthquake Engineering Research Center, "PEER Strong Motion Data Base", http://peer.berkeley.edu/smcat/ (2001).
6. PEER, Pacific Earthquake Engineering Research Center, "Open System for Earthquake Engineering Simulation (OpenSees)", http://opensees.berkeley.edu/ (2003).
7. Makris, N., C. J. Black. "Rocking Response of Equipment Anchored to a Base Foundation." PEER 2001/14, Pacific Earthquake Engineering Research Center, University of California, Berkeley (2001).
8. Chadwell, C.B., R. A. Imbsen. "XTRACT: A Tool for Axial Force - Ultimate Curvature Interactions", ASCE Structures Congress, Nashville, TN (2004). In Publication.